

## Novel Alkoxide Cluster Topologies Featuring Rare Seesaw Geometry at Transition Metal Centers

James A. Bellow,<sup>[a]</sup> Dong Fang,<sup>[a]</sup> Natalija Kovacevic,<sup>[a]</sup> Philip D. Martin,<sup>[a]</sup> Jason Shearer,<sup>\*[b]</sup> G. Andrés Cisneros,<sup>\*[a]</sup> and Stanislav Groysman<sup>\*[a]</sup>

Molecules with central atoms possessing a coordination number of four are commonplace in coordination chemistry.<sup>[1]</sup> The majority of four-coordinate compounds display either tetrahedral or square planar geometry. However, valence shell electron pair repulsion (VSEPR) theory predicts a third type of four-coordinate geometry—the seesaw, or sawhorse. Two possible cases of seesaw geometry can be distinguished—the *cis*-divacant octahedron (angles of 180° and 90°) and the monovacant trigonal bipyramidal (angles of 180°, 120°, and 90°).<sup>[2]</sup> Examples of seesaw geometry can be found in main-group compounds due to the repulsive presence of lone pairs.<sup>[3]</sup> Seesaw transition metal complexes are of interest, as they possess a vacant coordination site that enables substrate coordination and activation.<sup>[2]</sup> However, seesaw transition metal complexes are extremely rare, and the requirements toward their attainment are poorly understood.<sup>[4–9]</sup> Recent computational work by Alvarez and co-workers supports the plausibility of seesaw geometry for first-row transition elements.<sup>[10]</sup> In particular, it has been proposed that seesaw geometry at transition metal centers arises primarily for certain electron configurations, particularly for d<sup>6</sup> and closed-shell d<sup>10</sup> metal centers.<sup>[2,11]</sup> Herein we demonstrate the first example in which the same seesaw geometry is observed for the series of transition metals (Cr<sup>II</sup>–Co<sup>II</sup>) featuring varying electron configurations (d<sup>4</sup>–d<sup>7</sup>). This geometry is enabled by the unique combination of the steric bulk of the ancillary ligands, alkoxides, combined with the inclusion of lithium chloride in the structure. Density functional theory (DFT) calculations shed light on the bonding interactions in these complexes and give insight into their electronic structures.

The properties and the reactivity of alkoxide-ligated metal centers depend on the steric and electronic properties of the alkoxide.<sup>[12–15]</sup> Bulky ligands have been employed in

low-coordinate complexes containing a plethora of different transition metals, many of which have shown small molecule activation capabilities.<sup>[16–26]</sup> The majority of previously reported bulky alkoxide ligands contain three identical substituents. We combined two *tert*-butyl groups with a phenyl group, attempting to achieve directionality in the alkoxide coordination, thus inducing higher crystallinity. The ligand [OC(*t*Bu)<sub>2</sub>Ph] ([OR] henceforth) was prepared by the addition of phenyllithium to hexamethylacetone. The structure of the lithium salt of the ligand has been confirmed by X-ray structure determination. The ligand crystallizes as the trimer Li<sub>3</sub>(OR)<sub>3</sub> (**1**; see the Supporting Information for the crystal structure) from hexane, with two-coordinate geometry featured at the lithium centers.

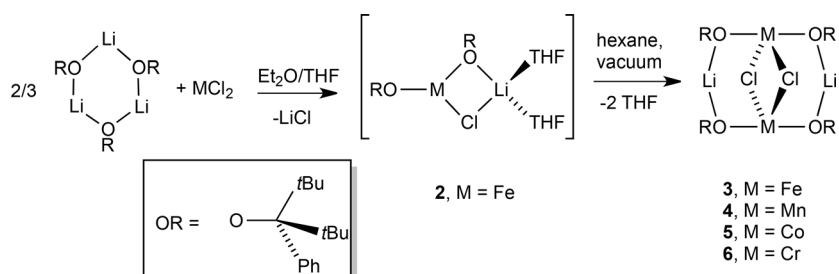
Addition of two equivalents of **1** to a solution of iron(II) chloride forms transiently the respective three-coordinate bis(alkoxide) complex, **2**, in solution. The compound is structurally similar to a chromium bis(alkoxide) complex previously reported by Power and co-workers.<sup>[27]</sup> Compound **2** is unstable in the absence of a coordinating solvent (THF).<sup>[28]</sup> Dissolution in hexanes and solvent removal under vacuum leads to the dissociation of THF ligands and subsequent dimerization, forming compound **3** (Scheme 1). Following similar protocols, the reactions of manganese(II) chloride, cobalt(II) chloride, and chromium(II) chloride with **1** form complexes **4–6**, respectively. Compounds **3–6** were characterized by X-ray crystallography. X-ray quality crystals of **3–6** were obtained upon recrystallization from hexanes at –35 °C. The structures of compounds **3** and **4** are depicted in Figure 1a and b; the structures of **2**, **5**, and **6** can be found in the Supporting Information. Complexes **3–6** are all isostructural clusters featuring an M<sub>2</sub>Li<sub>2</sub>Cl<sub>2</sub>(OR)<sub>4</sub> core.<sup>[29]</sup> Each chloride is bridging two transition metals. The lithium centers are two-coordinate as in the structure of **1**, whereas the transition metals are four-coordinate. A Crystal Structure Database search demonstrates that such a topology is unprecedented.<sup>[30]</sup> Further confirmation of the identical connectivity pattern in these structures comes from the virtually indistinguishable IR spectra of these complexes (Figure S8 in the Supporting Information).

Most significantly, dimeric complexes **3–6** all possess seesaw geometry at transition metal centers. The space-filling model of **3** (Figure 1c) shows the bulky *tert*-butyl and phenyl groups on the alkoxides forming a tight cage around the complex. Thus, we propose that the seesaw geometry

[a] J. A. Bellow, D. Fang, N. Kovacevic, Dr. P. D. Martin, Prof. G. A. Cisneros, Prof. S. Groysman  
Wayne State University, Detroit, MI 48202 (USA)  
E-mail: andres@chem.wayne.edu  
groysman@chem.wayne.edu

[b] Prof. J. Shearer  
Department of Chemistry, University of Nevada  
Reno, NV 89557 (USA)  
E-mail: shearer@unr.edu

 Supporting information for this article is available on the WWW under <http://dx.doi.org/10.1002/chem.201302558>.



Scheme 1. Synthesis of compounds **2–6**.

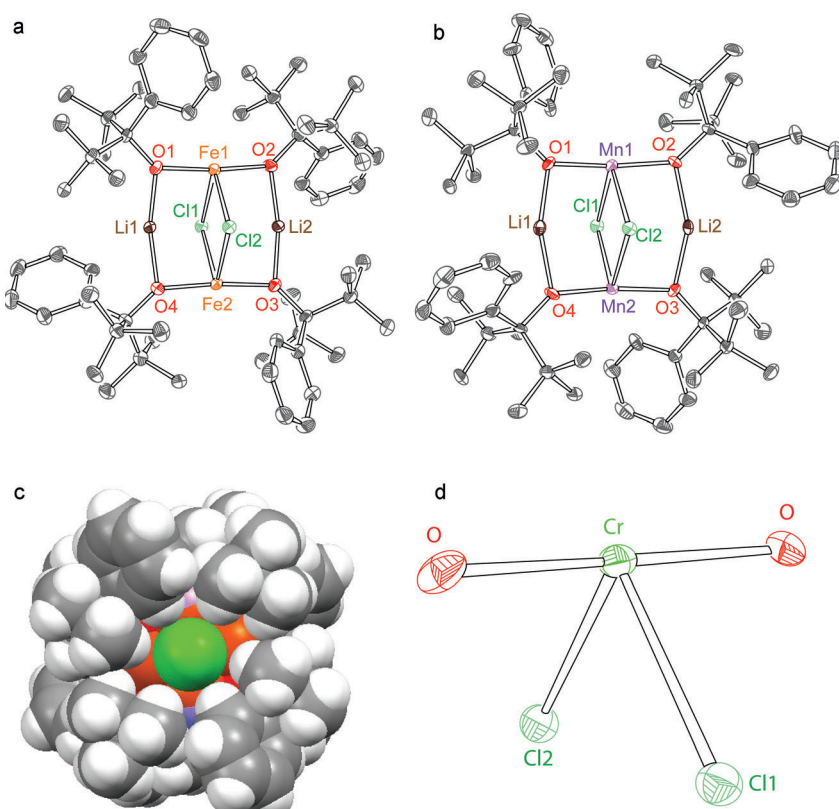


Figure 1. a) Crystal structure of **3**. b) Crystal structure of **4**. c) Space-filling model of **3**. d) Structure of seesaw core with O-M-O and Cl-M-Cl angles. For the crystal structures of **3** and **4**, 50% probability ellipsoids are shown. Hydrogen atoms are omitted for clarity. Selected bond lengths [Å] and angles [°] for **3**: Fe1–O1 1.904(4), Fe1–O2 1.917(4), Fe1–Cl1 2.474(2), Fe1–Cl2 2.520(2), O1–Fe1–O2 173.8(2), Cl1–Fe1–Cl2 86.96(8)°.

arises in part due to the steric bulk of the alkoxide ligands. The immediate coordination environment of the transition metals is presented in Figure 1d. The O–M–O angles of the complexes range from 171° to 176°, and the Cl–M–Cl angles are all within the 84°–88° range. The M–Cl distances in each complex are similar to those in related complexes, confirming that there are M–Cl bonds in these structures.<sup>[22,27,31]</sup> In addition, the Li–Cl distances range from 2.5–3.0 Å, which are longer than those for Li–Cl bonds in related structures.<sup>[22,27,31]</sup>

To confirm that the structures obtained by single crystal diffraction analysis are representative of the bulk material, complexes **3**, **4** and **5** were subjected to metal K-edge X-ray

absorption spectroscopy. The XANES region of the X-ray absorption spectra (XAS) all display pre-edge features corresponding to nominal 1s→3d transitions. The pre-edge feature of **3** has a peak-area of 8.2(1) % eV relative to the edge height (Figure 2a). Although the geometry about the Fe<sup>II</sup> center is unprecedented, we can think of the Fe<sup>II</sup> center as contained in a pseudotrigonal bipyramidal structure. We find that the area under this feature compares well with other 5-coordinate Fe<sup>II</sup> complexes, and is thus consistent with the seesaw geometry.<sup>[32]</sup>

High resolution ( $k=2.0\text{--}17.5\text{ \AA}^{-1}$ ) EXAFS analysis of the XAS is also consistent with the crystallographic structure of **3**. In addition to the two Fe–O (1.89 Å), two Fe–Cl (2.48 Å) and one Fe–Fe (3.60 Å) vectors, there were also a plethora of multiple scattering (MS) pathways that needed to be accounted for to properly solve the EXAFS (Figure 2b). These MS pathways are strongly dependent on the O–Fe–O and Cl–Fe–Cl bond angles. A best fit to the data yields an O–Fe–O bond angle of 174° and a Cl–Fe–Cl bond angle of 86°. Thus, the results are consistent with the crystallographic data. Analysis of the XAS for complexes **4** and **5** yield similar fits to the data (see the Supporting Information).

Continuous symmetry measurements provide a useful handle to evaluate the geometry of the metal center.<sup>[33,34]</sup> The continuous symmetry values have been calculated using the method detailed by Cicera, Alemany, and Alvarez in the Shape2 software.<sup>[2]</sup> The continuous symmetry values for the crystal (computationally optimized) structures (**3–6**) are 2.2 (2.6), 2.2 (2.4), 2.0 (2.9) and 2.1 (2.5), respectively. As the continuous symmetry values range from 0 to 100 (0 means perfect seesaw, whereas 100 means totally distorted), both crystal and computational structures present geometry close to that of a perfect seesaw.

To shed light on the bonding and the electronic structure of these unusual molecules, we conducted DFT calculations

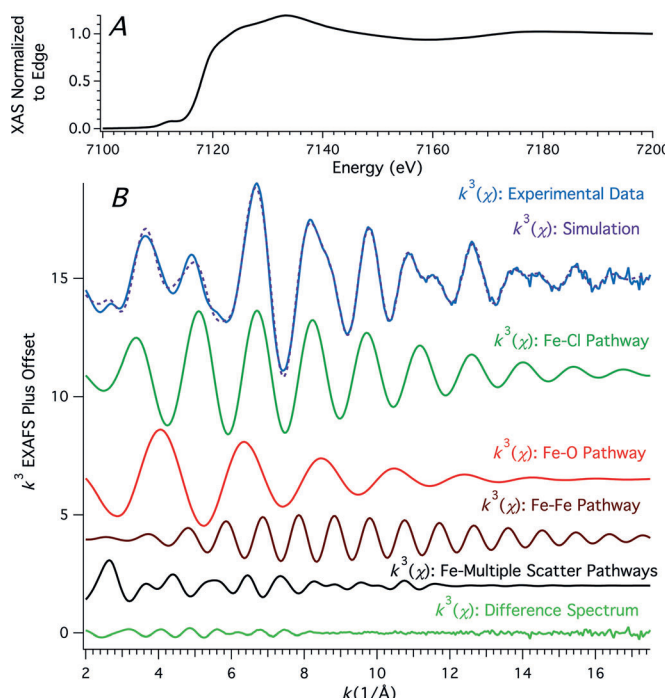


Figure 2. a) XANES region of the Fe K-edge XAS for compound 3. b) The  $k^3(\chi)$  plots of the experimental data, best fit, deconvolved scattering pathways and residual for 3.

(see the Supporting Information for Computational Methods) on the simplified models of **3–6** (*t*Bu groups replaced by Me groups). The superposition of the calculated and crystal structures shows good agreement between them (Figure S16 in the Supporting Information).<sup>[35]</sup> Combined electron localization function (ELF)<sup>[36]</sup>/noncovalent interaction (NCI)<sup>[37,38]</sup> analysis<sup>[39–41]</sup> was performed to gain a better understanding of interatomic interactions (see the Supporting Information for ELF results). NCI describes interatomic interactions by peaks of the reduced electron density gradient at low electron densities. Taking **6** as an example, the strong metal–ligand (Cr–O and Cr–Cl) interaction is evidenced by the blue NCI surfaces in Figure 3a. In addition, the surface for Cr–O (circled in black) has a darker blue color than the surface for Cr–Cl (circled in red), indicating that the interaction between Cr and Cl is slightly weaker than between Cr and O. Moreover, the interaction between Li and Cl is much weaker than the one between Cr and Cl as demonstrated by the green surfaces (circled in yellow). Next, we replaced the alkyl substituents R of the OR groups by hydrogen atoms to investigate their effect on the stability of the seesaw geometry in the core. Although the optimized Cr complex did not retain the seesaw geometry, the other (Mn–Co) complexes were found to only undergo slight distortion (Figure S20 in the Supporting Information). These results underscore the importance of lithium–oxygen interactions (circled in blue) in these structures for the stabilization of the seesaw core. To determine the steric effect of the [*t*Bu<sub>2</sub>(Ph)CO] ligand, we carried out the NCI analysis on the full crystal structure of **6** (unoptimized, Figure 3b). Some of

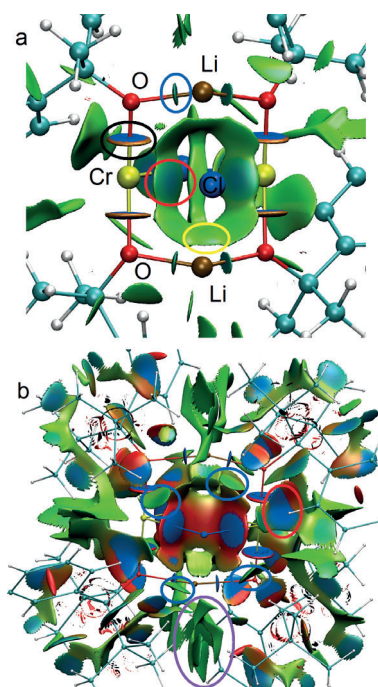


Figure 3. NCI surfaces for complex **6**, the isovalue is 0.5. a) The optimized structure with *tert*-butyl was replaced by methyl (only the core is shown),  $-0.07 < \text{sign}(\lambda_2)\rho < -0.07$  a.u. b) NCI analysis for the complete (unoptimized) crystal structure,  $-0.02 < \text{sign}(\lambda_2)\rho < 0.02$  a.u. Regarding the chosen arbitrary color code, red surface indicates strong repulsion; blue surface indicates strong attraction; green surface indicates relatively weak interactions. Different  $\text{sign}(\lambda_2)\rho$  ranges may be used to distinguish the strength of the interactions. Note that one can compare the relative strength of the interactions based on the colors only when using the same  $\text{sign}(\lambda_2)\rho$  range.

the notable interactions include a weak attraction between Cr and *ortho*-H (circled in red), and a weak attraction between Cl and H (*t*Bu) atoms (circled in blue). Similar interactions are also present in the optimized simplified structures bearing Me substituents (Figure S18 in the Supporting Information). However, the full structure also demonstrates a weak attraction between the *t*Bu groups and neighboring phenyl group (circled in violet). This interaction may be responsible for the formation of the cage-like structure (Figure 1c).

We carried out a preliminary investigation of the magnetic properties of **3–6**. To probe the solution state effective magnetic moments of **3–6**, the Evans method was conducted at room temperature.<sup>[42]</sup> The largest effective magnetic moment observed was that of **4**, which was observed to be 11.6  $\mu\text{B}$ . The expected spin-only magnetic moment for two uncoupled Mn<sup>II</sup> centers is 11.0  $\mu\text{B}$ . The calculated and observed values were also similar for complexes **3** (8.8  $\mu\text{B}$ , calcd 8.9  $\mu\text{B}$ ), **5** (7.8  $\mu\text{B}$ , calcd 6.9  $\mu\text{B}$ ), and **6** (8.4  $\mu\text{B}$ , calcd 8.9  $\mu\text{B}$ ). We have also conducted SQUID magnetometry on compound **3**, featuring the largest number of unpaired electrons (Figure S5 in the Supporting Information). SQUID data are fully consistent with solution measurements. At room temperature, a magnetic moment of 11.6  $\mu\text{B}$  ( $\chi T = 16.8 \text{ cm}^3(\text{mol K})^{-1}$ ) is observed, indicating two uncoupled

metal centers. At low temperatures,  $\chi T$  values drop to about 0, indicating antiferromagnetic coupling.

In summary, we have synthesized novel clusters supported by bulky alkoxide ligands featuring a  $M_2Li_2Cl_2(OR)_4$  core ( $M=Cr-Co$ ). These clusters exhibit the highly unusual seesaw geometry at the transition metal centers. Our current focus is on the synthesis of neutral two-coordinate bis(alkoxide) complexes using these dimers as precursors and the investigation of their reactivity.

CCDC-939862 (**1**), 939863 (**2**), 939864 (**3**), 939865 (**4**), 939866 (**5**), and 939867 (**6**) contain the supplementary crystallographic data for this paper. These data can be obtained free of charge from The Cambridge Crystallographic Data Centre via [www.ccdc.cam.ac.uk/data\\_request/cif](http://www.ccdc.cam.ac.uk/data_request/cif).

## Acknowledgements

We acknowledge Wayne State University for the start-up funding. The computing time from Wayne State C&IT is gratefully acknowledged. We thank Prof. D. Freedman and Michael Graham (Northwestern University) for the help with SQUID measurements. We also acknowledge Prof. P. L. Holland (Yale University) for the insightful discussions.

**Keywords:** alkoxides • cluster compounds • continuous symmetry measures • seesaw geometry • transition metals

- [1] N. N. Greenwood, A. Earnshaw, *Chemistry of the Elements*, 2<sup>nd</sup> ed., Pergamon, Oxford, **1997**, pp. 912–914.
- [2] J. Cicera, P. Alemany, S. Alvarez, *Chem. Eur. J.* **2004**, *10*, 190–207.
- [3] P. Atkins, T. Overton, J. Rourke, M. Weller, F. Armstrong, *Inorganic Chemistry*, 4th ed., W. H. Freeman and Company, New York, **2006**, pp. 45–48.
- [4] W. Baratta, E. Hertweck, P. Rigo, *Angew. Chem.* **1999**, *111*, 1733–1735; *Angew. Chem. Int. Ed.* **1999**, *38*, 1629–1631.
- [5] D. Huang, W. E. Streib, J. C. Bollinger, K. C. Caulton, R. F. Winter, T. Scheiring, *J. Am. Chem. Soc.* **1999**, *121*, 8087–8097.
- [6] F. Bonhomme, K. Yvon, G. Triscone, K. Jansen, G. Auffermann, P. Mueller, W. Brönger, P. Fischer, *J. Alloys Compd.* **1992**, *178*, 161–166.
- [7] D. M. Lunder, E. B. Lobkovsky, W. E. Streib, K. C. Caulton, *J. Am. Chem. Soc.* **1991**, *113*, 1837–1838.
- [8] T. J. Hubin, N. W. Alcock, D. H. Busch, *Acta Crystallogr. Sect. C* **2000**, *56*, 37–39.
- [9] R. K. Minhas, J. J. H. Edema, S. Gambarotta, A. Meetsma, *J. Am. Chem. Soc.* **1993**, *115*, 6710–6717.
- [10] J. Cicera, E. Ruiz, S. Alvarez, *Inorg. Chem.* **2008**, *47*, 2871–2889.
- [11] M. Oliván, E. Clot, O. Eisenstein, K. C. Caulton, *Organometallics* **1998**, *17*, 3091–3100.
- [12] P. T. Wolczanski, *Polyhedron* **1995**, *14*, 3335–3362.
- [13] P. T. Wolczanski, *Chem. Commun.* **2009**, 740–757.
- [14] P. P. Power, *J. Organomet. Chem.* **2004**, *689*, 3904–3919.
- [15] S. A. Cantalupo, J. S. Lum, M. C. Buzzo, C. Moore, A. G. DiPasquale, A. L. Rheingold, L. H. Doerrer, *Dalton Trans.* **2010**, *39*, 374–383.
- [16] M. Bochmann, G. Wilkinson, G. B. Young, M. B. Hursthouse, K. M. A. Malik, *J. Chem. Soc. Dalton Trans.* **1980**, 1863–1871.
- [17] R. E. LaPointe, C. P. Schaller, P. T. Wolczanski, J. F. Mitchell, *J. Am. Chem. Soc.* **1986**, *108*, 6382–6384.
- [18] D. R. Neithamer, R. E. LaPointe, R. A. Wheeler, D. S. Richeson, G. D. Van Duyne, P. T. Wolczanski, *J. Am. Chem. Soc.* **1989**, *111*, 9056–9072.
- [19] J. J. Curley, A. F. Cozzolino, C. C. Cummins, *Dalton Trans.* **2011**, *40*, 2429–2432.
- [20] C. Schwarzmaier, A. Noor, G. Glatz, M. Zabel, A. Y. Timoshkin, B. M. Cossairt, C. C. Cummins, R. Kempe, M. Scheer, *Angew. Chem.* **2011**, *123*, 7421–7424; *Angew. Chem. Int. Ed.* **2011**, *50*, 7283–7286.
- [21] B. D. Murray, P. P. Power, *J. Am. Chem. Soc.* **1984**, *106*, 7011–7015.
- [22] M. M. Olmstead, P. P. Power, G. Sigel, *Inorg. Chem.* **1986**, *25*, 1027–1033.
- [23] R. A. Bartlett, J. J. Ellison, P. P. Power, S. C. Shoner, *Inorg. Chem.* **1991**, *30*, 2888–2894.
- [24] M. M. Rodriguez, E. Bill, W. W. Brennessel, P. L. Holland, *Science* **2011**, *334*, 780–783.
- [25] S. Groysman, D. Villagrán, D. Freedman, D. G. Nocera, *Chem. Commun.* **2011**, *47*, 10242–10244.
- [26] M. B. Chambers, S. Groysman, D. Villagrán, D. G. Nocera, *Inorg. Chem.* **2013**, *52*, 3159–3169.
- [27] J. Hvoslef, H. Hope, B. D. Murray, P. P. Power, *J. Chem. Soc. Chem. Commun.* **1983**, 1438–1439.
- [28] We were able to obtain crystals of **2** from a mixture of hexanes and a small amount of THF. It co-crystallizes with **3**. The crystals are unstable, rapidly deteriorating even in the absence of air (covered by Paratone oil).
- [29] The complexes display transition metal/lithium disorder in the core. The disorder has been satisfactorily modeled so that in a given configuration the transition metals occupy positions *trans* to each other. The remaining two positions are occupied by lithium atoms.
- [30] Somewhat related topologies are observed, but none replicates all of the structural features found in **3–6**. For selected examples, see:
  - a) Y. K. Gun'ko, U. Cristmann, V. G. Kessler, *Eur. J. Inorg. Chem.* **2002**, 1029–1031; b) C. E. Anson, W. Klopper, J.-S. Li, L. Ponikiewski, A. Rothenberger, *Chem. Eur. J.* **2006**, *12*, 2032–2038; c) D. J. Gallagher, K. W. Henderson, A. R. Kennedy, C. T. O'Hara, R. E. Mulvey, R. B. Rowlings, *Chem. Commun.* **2002**, 376–377; d) K. J. Drewette, K. W. Henderson, A. R. Kennedy, R. E. Mulvey, C. T. O'Hara, R. B. Rowlings, *Chem. Commun.* **2002**, 1176–1177; e) A. R. Kennedy, J. Klett, R. E. Mulvey, S. Newton, D. S. Wright, *Chem. Commun.* **2008**, 308–310; f) R. E. Mulvey, *Dalton Trans.* **2013**, *42*, 6676–6693.
- [31] N. A. Eckert, J. M. Smith, R. J. Lachicotte, P. L. Holland, *Inorg. Chem.* **2004**, *43*, 3306–3321.
- [32] C. R. Randall, L. Shu, Y.-M. Chiou, K. S. Hagen, M. Ito, N. Kitajima, R. J. Lachicotte, Y. Zang, L. Que, Jr., *Inorg. Chem.* **1995**, *34*, 1036–1039.
- [33] H. Zabrodsky, S. Peleg, D. Avnir, *J. Am. Chem. Soc.* **1992**, *114*, 7843–7851.
- [34] M. Pinsky, D. Avnir, *Inorg. Chem.* **1998**, *37*, 5575–5582.
- [35] Root mean squared deviation (RMSD) with respect to the crystal structures for **3–6** are 0.34, 0.15, 0.18 and 0.22 Å, respectively.
- [36] B. Silvi, A. Savin, *Nature* **1994**, *371*, 683–686.
- [37] E. R. Johnson, S. Keinan, P. Mori-Sánchez, J. Contreras-García, A. J. Cohen, W. Yang, *J. Am. Chem. Soc.* **2010**, *132*, 6498–6506.
- [38] J. Contreras-García, E. R. Johnson, S. Keinan, R. Chaudret, J.-P. Piquemal, D. N. Beratan, W. Yang, *J. Chem. Theory Comput.* **2011**, *7*, 625–632.
- [39] N. Gillet, R. Chaudret, J. Contreras-García, W. Yang, B. Silvi, J.-P. Piquemal, *J. Chem. Theory Comput.* **2012**, *8*, 3993–3997.
- [40] D. Fang, R. Chaudret, J.-P. Piquemal, G. A. Cisneros, *J. Chem. Theory Comput.* **2013**, *9*, 2156–2160.
- [41] D. Fang, R. L. Lord, G. A. Cisneros, *J. Phys. Chem. B* **2013**, *117*, 6410–6420.
- [42] D. F. Evans, *J. Chem. Soc.* **1959**, 2003–2005.

Received: July 2, 2013

Published online: August 9, 2013